Available online at www.sciencedirect.com
SCIENCE DIRECT®
Applied Catalysis A: General 258 (2004) 203–214
APPLIED CATALYSIS A: GENERAL
www.elsevier.com/locate/apcata

Water-gas shift: comparative screening of metal promoters for metal/ceria systems and role of the metal

Gary Jacobs, Emilie Chenu, Patricia M. Patterson, Leann Williams, Dennis Sparks, Gerald Thomas, Burtron H. Davis*

Center for Applied Energy Research, University of Kentucky, 2540 Research Park Drive, Lexington, KY 40511, USA

Received 6 June 2003; received in revised form 29 August 2003; accepted 3 September 2003

Abstract

In situ diffuse reflectance mode (DRIFTS) measurements for adsorption of CO and under the water-gas shift (WGS) reaction revealed that formates emerge on the surface of reduced ceria after the reaction of CO with geminal OH groups. These groups are formed after reduction of the ceria surface shell. X-ray absorption near edge spectroscopy (XANES) results demonstrated that the process of surface shell reduction was strongly catalyzed by the presence of metal, while changing very little, if at all, the catalysis of bulk ceria reduction. For 1% Pt/ceria, under steady state WGS at a high H_2O/CO ratio, surface formate concentrations were strongly limited at high CO conversions, while Pt-CO was affected only slightly. Under high H_2O/CO ratios, CO exhibits a first order rate dependency, and therefore, the active site is expected to move to sparser coverages of CO, which suggested that the WGS mechanism likely proceeded via formates. Later, XANES work gave no evidence for the reoxidation of ceria surface by water under a hydrogen environment, which would be necessary to substantiate an alternate mechanism, referred to as the ceria-mediated redox process. Later, isotope switching from H_2O to D_2O was carried out to validate the possibility that decomposition of surface formates could be the rate limiting step for the mechanism, as was proposed and demonstrated earlier by Shido and Iwasawa. In agreement with their findings, we also observed a normal isotope effect, consistent with a link between the activation energy barrier of the rate limiting step to the breaking of the C–H bond of the formate.

In this study, a variety of metals were screened to try to gain further insight into the role played by the metal in the catalysis of metal/ceria systems for WGS. One group of metals was selected on the basis of reduction temperature, since spillover from reduced metal likely catalyzes the reduction of ceria surface. Therefore, we tested the following metals, moving from lowest to highest reduction temperature: Pt < Ni < Co = Fe. These were found to catalyze reduction of ceria surface by the same trend, as well as the WGS rate. In each case, DRIFTS showed that as reduction of ceria surface occurred, marked increases in geminal OH intensities occurred, which yielded formates upon adsorption of CO. The second group of metals was a comparative study between Pt and Group 11 metals that have been purported to catalyze surface reduction at the same or even lower temperatures than Pt. Indeed, the surface reduction occurred at a lower temperature than for Pt with Au and at a similar temperature with Cu. However, on an equivalent atomic basis, the depth of reduction of ceria was found to be higher when Pt was used over Au, and the WGS rate was about 20 times higher with Pt than by Group 11 metal promotion at 250 °C and higher. WGS feed conditions were carefully chosen to mimic conditions found in a fuel cell reformer.

Keywords: Water-gas shift; LTS; Ceria; Platinum; Gold; Nickel; Copper; Iron; Cobalt; DRIFTS

1. Introduction

Proton exchange membrane fuel cells (PEMFC) using hydrogen may replace the internal combustion engine in the future and revolutionize the transportation sector. However, before any gain in efficiency or environmental benefit can be realized from PEMFC, hydrogen of sufficient purity must be generated [1–3]. CO is especially problematic, as parts per million levels poison noble metal catalysts used in the fuel cell. The product stream from reforming contains about 8–10% CO, and these levels are converted to about 3–5% by high-temperature water-gas shift (HTS) run at near equilibrium conditions [4]. Low-temperature water-gas shift (LTS) can be used after the HTS step to achieve even higher conversions, but effective catalysts must be designed so that, in conjunction with preferential oxidation (PROX)

* Corresponding author. Tel.: +1-859-257-0251; fax: +1-859-257-0302.
E-mail address: davis@caer.uky.edu (B.H. Davis).

0926-860X/$ – see front matter © 2003 Elsevier B.V. All rights reserved.
doi:10.1016/j.apcata.2003.09.007

to convert CO to CO_2, levels in the ppm range can be achieved.

One catalyst system receiving considerable attention recently for LTS is ceria loaded with metal promoters, such as platinum. It is anticipated that, with proper development, metal promoted ceria catalysts should realize much higher CO conversions than even commercial CuZnO catalysts. There is currently an ongoing debate in the academic community as to the roles played by ceria and the metal in promoting the water-gas shift (WGS) reaction. The redox mechanism and oxygen storage capacity of ceria is usually claimed, where the metal plays a direct role in the mechanism of the WGS reaction [5–8]:

Ceria-mediated redox process:

$$* + CO \Rightarrow *\text{-}CO$$

$$*\text{-}CO + 2CeO_2 \Rightarrow Ce_2O_3 + CO_2 + *$$

$$H_2O + Ce_2O_3 \Rightarrow H_2 + 2CeO_2$$

Formate Mechanism:

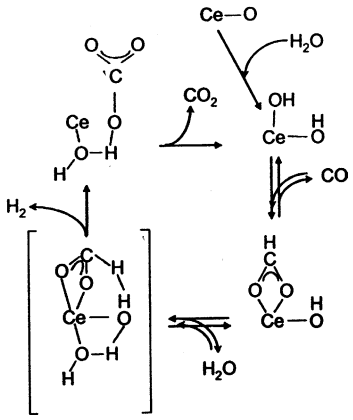

However, there are a number of observations, both past and present, that have been made that are in sharp disagreement to the above process. These observations served as a basis for a mechanism proceeding through surface formates [9,10], shown above. The formates arise by reaction of geminal OH functional groups that are present on the reduced surface of ceria with CO [9–11]. Water addition then decomposes the surface formate to liberate H_2 and CO_2, the latter of which may proceed via a surface carbonate [9,10]. Shido and Iwasawa [9,10] postulated the above mechanism as one possibility, and additional studies are needed to validate each step of the pathway.

The initial tests for both systems were conducted on catalysts that were not optimized. Recently, we have attempted to validate the appropriate mechanism while utilizing ceria with higher surface area (SA) than used in those previous studies, and that made it amenable to spectroscopic studies. The ceria was made using the urea precipitation–gelation method of Li et al. [7], and Fu and Weber [8], which is an adaptation of the work of Amenomiya et al. [12].

We have utilized in situ Fourier transform infrared spectroscopy (FTIR) in the diffuse reflectance mode (DRIFTS) to examine the surface of Pt promoted CeO_2 catalysts after adsorption of the different reactants (CO and H_2O) and during steady state reaction testing of the water-gas shift reaction. In preliminary studies utilizing a high H_2O/CO ratio, Pt loaded ceria catalysts were examined [13,14] and it was found that not only did addition of CO to reduced ceria surface generate significant formate bands, the formates were rate limited by the water-gas shift reaction. In contrast, the Pt–CO band displayed very little change under reaction. We then compared those findings to the rate law for metal promoted ceria catalysts obtained from kinetic studies [7], which follows:

$$\text{rate} = \frac{k_1 k_2 P_{CO} P_{H_2O}}{k_1 P_{CO} + k_2 P_{H_2O}}$$

According to the rate expression, CO exhibits a first order partial pressure dependency at high H_2O/CO ratios, and therefore, the adsorbed CO species that is the intermediate should move to sparser coverages with increasing conversion (i.e. higher reaction rates). Therefore, according to our previous results, only the formate mechanism satisfied the kinetic and IR criteria.

Reexamining the IR work of Hilaire et al. [6], measurements were conducted on a Pt/ceria catalyst under water-gas shift at a high CO/H_2O ratio, where a zero order dependency of the WGS rate for P_{CO} is expected, and this is due to saturation of the active site. Interestingly, both saturation of Pt with CO and saturation of ceria by "carbonates" was reported. Based on our findings, we suggest that the OCO vibrations reported as carbonates were actually formates, as previously discussed. The zero order dependency of CO at high CO/H_2O ratios could therefore be easily attributed to the formate mechanism as well. This underscores the need to test catalysts at high H_2O/CO ratios, where the first order CO rate dependency could differentiate between an active site based on Pt or one based on the geminal hydroxyl groups of ceria. Since only the formates were found to be rate limited, the results suggested strongly that the mechanism passed through a formate intermediate.

In a separate investigation, X-ray absorption near edge spectroscopy (XANES) work [15,16] revealed that reduced surface ceria did not reoxidize when water was introduced to

the hydrogen stream under the reducing atmosphere. Such a reoxidation would be necessary for the ceria-mediated redox process to be substantiated under the hydrogen-rich conditions found in a fuel cell reformer.

We tested the merits of the formate mechanism by attempting to improve the active site densities based on the ceria surface function [14]. The loading of metal (Pt) promoter was kept constant at 1% by weight because, based on our previous studies with reduction promoters, 1% should be enough to achieve the catalysis of surface ceria reduction, and thereby generate the active geminal OH groups, the catalytically active sites of the proposed formate mechanism. The surface area of ceria was varied by various means, and results of catalytic testing and IR indicated a direct correlation between the ceria surface area and the generation of surface formates after surface reduction. We established that the surface formates could provide an important indicator for the catalyst activity. In the previous work of Li et al. [7], an attempt was made to improve the catalytic activity by increasing the metal–ceria interface by using higher loadings. In that case, the ceria-mediated redox mechanism served as a model, and the metal used was Cu. Interestingly, formulations with metal loadings between 5 and 40% showed no improvement in the activity [7].

More recently, we carried out isotope switching from H_2O to D_2O to try to either validate or discredit the possibility that decomposition of surface formates could be the rate limiting step for the mechanism, as was proposed and demonstrated earlier by Shido and Iwasawa [9,10]. Testing was carried out in an in situ DRIFTS cell so that the hydrogen and deuterium forms of formate could be followed. Conversion was monitored by GC. In agreement with their findings, we also observed a normal isotope effect, consistent with a link between the activation energy barrier of the rate limiting step to the breaking of the C–H bond of the formate [15].

In this investigation, it was deemed appropriate to screen a series of selected metals on the same high surface area ceria. The first reason was to determine the effectiveness of other metals in comparison to Pt in promoting the reduction of ceria, which is required for either mechanism. In that way, a cheaper alternate metal might be found. The second was to observe how surface formate concentrations responded at different reduction temperatures for each of the catalytic materials screened. Metals were added at the same atomic loading.

2. Experimental

2.1. Catalyst Preparation

High surface area ceria was prepared via homogeneous precipitation of the nitrate in urea with aqueous ammonia in a similar manner to Li et al. [7]. The idea is an adaptation of work conducted on CuO-ZrO_2 methanol synthesis catalysts [12], whereby urea decomposition is a process resulting in a slower, more homogeneous precipitation. On a basis of 30 g CeO_2, an appropriate amount of $Ce(NO_3)_3{\cdot}6H_2O$ (Alfa Aesar, 99.5%) and 240 g urea (Alfa Aesar, 99.5%) were dissolved in 900 ml of deionized water, and to the solution about 30 ml NH_4OH (Alfa Aesar, 28–30% NH_3) was added dropwise (∼1 ml/min). The mixture was then boiled at 100 °C with constant stirring. The precipitate was filtered, washed with 600 ml of boiling deionized water, and dried in an oven (100 °C) overnight. The dried precipitate was then crushed and calcined in a muffle furnace at 400 °C for 4 h. This support is designated HSAUP.

The support has a BET surface area of 105 m^2/g. Platinum was added via incipient wetness impregnation (IWI) with tetraammine platinum(II) nitrate solution. Likewise, copper, nickel, iron, and cobalt were also added by IWI of the nitrate. Gold was added following the precipitation method found in [8], utilizing $HAuCl_4$. Catalysts were calcined at 400 °C for 4 h after metal component addition.

Low surface area ceria (designated LSAP) was prepared by the standard homogeneous precipitation method using cerium nitrate and aqueous ammonia, and the preparation is reported elsewhere [14].

2.2. BET surface area

BET Surface Area measurements were carried out in a Micromeritics Tristar 3000 gas adsorption analyzer. In each trial, a weight of approximately 0.25 g of sample was used. The adsorptive gas was nitrogen (N_2) and the adsorption was carried out at the boiling temperature of liquid nitrogen.

2.3. X-ray diffraction

Powder diffractograms on calcined catalysts were recorded using a Philips X'Pert diffractometer. First, short times were used over a long range to ensure that CeO_2 had formed. The conditions were as follows: scan rate of 0.025° per step, scan time of 5 s per step over a 2θ range of 20–100°. Then, long times were used over a short range in order to quantify the CeO_2 domain size using line broadening analysis. The conditions employed for the latter were: scan rate of 0.025° per step, scan time of 30 s per step over a 2θ range of 20–40°. Similar scans were also conducted on the metal loaded catalysts.

2.4. Temperature programmed reduction

TPR was conducted on CeO_2 supports and metal promoted catalysts in a Zeton-Altamira AMI-200 unit, which was equipped with a thermal conductivity detector (TCD). Argon was used as the reference gas, and 10% H_2 (balance Ar) was flowed at 30 cc as the temperature was increased from 50 to 800 °C at a ramp rate of 10 °C/min. A liquid

nitrogen trap was used to capture any water that evolved from the catalyst prior to entering the TCD.

2.5. Diffuse reflectance infrared Fourier transform spectroscopy (DRIFTS)

A Nicolet Nexus 870 was used, equipped with a DTGS–TEC detector. A high-pressure/high-temperature chamber fitted with ZnSe windows was utilized as the WGS reactor for in situ reaction measurements. The gas lines leading to and from the reactor were heat traced, insulated with ceramic fiber tape, and further covered with general purpose insulating wrap. Scans were taken at a resolution of 4 to give a data spacing of 1.928 cm^{-1}. Typically, 128 scans were taken to improve the signal to noise ratio. The sample amount was 15 mg of powder.

A steam generator consisted of a downflow tube packed with quartz beads and quartz wool heated by a ceramic oven and equipped with an internal thermocouple. The lines after the steam addition were heat traced. The steam generator and lines were run at the same temperature as that at the in situ sample holder of the DRIFTS cell. This allowed us to accurately bring the reactants to the desired reaction temperature. Water was added to the steam generator by a thin needle welded to a 1/16th in. line. Two precision ISCO Model 500D syringe pumps were used to feed the water and deuterated water, and the system was equipped with a selector valve.

Feed gases were controlled by using Brooks 5850 series E mass flow controllers. Iron carbonyl traps consisting of lead oxide on alumina (Calsicat) were placed on the CO gas line. All gas lines were filtered with Supelco O_2/moisture traps. A schematic of the DRIFTS/reaction system is displayed in Fig. 1.

Activity tests were conducted at atmospheric pressure using a 1.27 cm stainless steel tubular reactor heated by an electric oven. Catalysts were diluted with silica beads (one part catalyst, three parts silica). The feed gas mixture was 1.6% CO, 42% H_2, 52% H_2O, balance N_2. For the Pt/CeO_2 catalyst, the contact times used were 0.0083 and 0.166 g s/cm^3, respectively, while the latter condition was used for the other metals. The same gas delivery system and pump was used for reaction testing as was used for DRIFTS. Water was knocked out using a molecular sieve prior to online analysis with an SRI 8610C GC. The GC includes two columns (15.2 cm silica gel packed and 7.62 cm molecular sieve) and two detectors (FID and TCD).

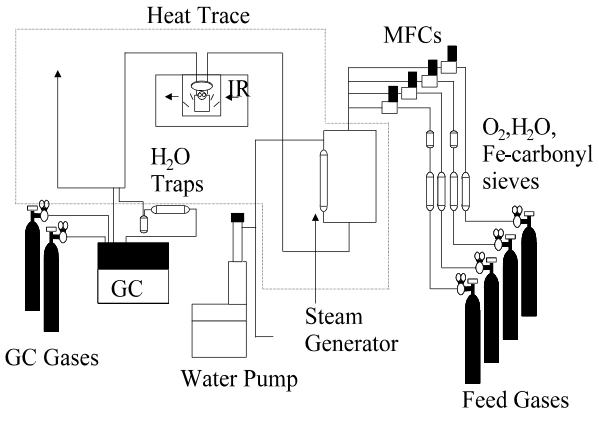

Fig. 1. In situ DRIFTS adsorption/reaction system.

To improve the sensitivity of the CO and CO_2 signals, the GC utilizes a methanizer, so that these product can be analyzed by FID. Conversion was calculated based on FID signals of CH_4. An internal N_2 standard provided a check based on the CO/N_2 ratio. Catalysts were activated with hydrogen at each condition.

2.6. X-ray absorption near edge spectroscopy

XANES spectra at the Ce L_{III} edge were recorded at the National Synchrotron Light Source (NSLS) at Brookhaven National Laboratory (BNL) in Upton, New York at beamline X18b. The X-rays were tuned by a Si(1 1 1) double crystal monochromator, which was detuned slightly to prevent glitches from harmonics. The catalyst was mixed with boron nitride and gently pressed into a disk and loaded into an in situ XAS cell. The samples were treated with hydrogen/helium at increasing reduction temperatures. The UHP H_2 and UHP He gases were mixed in a manifold and passed through an oxygen/water trap prior to entering the cell. Several scans of the catalyst samples were obtained and the spectra averaged to improve the signal to noise ratio.

3. Results and discussion

3.1. Standard characterization

BET surface areas are reported in Table 1. The HSAUP ceria support gave a more than two-fold improvement to the ceria prepared by homogeneous precipitation without urea. The ability to produce high surface area ceria was crucial for conducting studies using XANES spectroscopy at the cerium

Table 1
BET surface area, porosity, and composition results for supports and catalysts

Description	Metal (moles/100 g catalyst)	BET SA (m^2/g)	Pore volume (cm^3/g)	Radius (nm)
Support				
LSAP	–	42.8	0.137	8.80
1% Pt/LSAP	0.00513	37.9	0.121	6.37
HSAUP	–	105.5	0.121	2.29
1% Pt/HSAUP	0.00513	99.6	0.115	2.32
0.30% Ni/HSAUP	0.00513	99.5	0.118	2.38
0.33% Cu/HSAUP	0.00513	108.4	0.123	2.27
0.30% Co/HSAUP	0.00513	107.1	0.125	2.33
0.29% Fe/HSAUP	0.00513	100.5	0.119	2.38
1% Au/HSAUP	0.00513	102.2	0.120	2.35

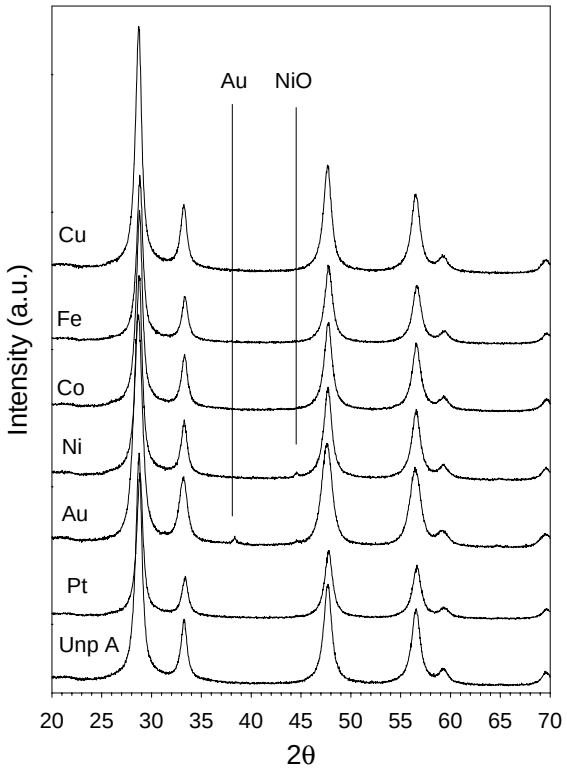

Fig. 2. XRD profiles of ceria and metal/ceria catalysts.

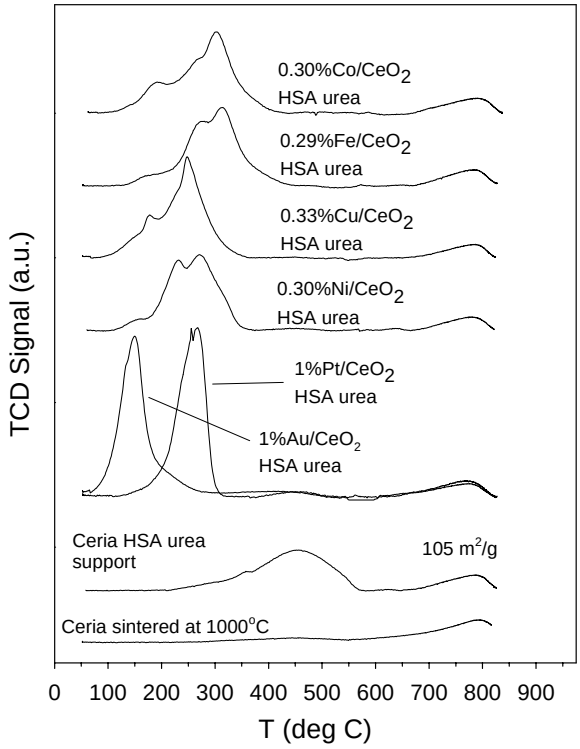

Fig. 3. TPR profiles of ceria sintered at 1000 °C, HSAUP ceria, and metal loaded ceria catalysts.

L_{III} edge, since the method averages over all the Ce atoms (surface and bulk). Previous attempts to conduct XANES experiments using the lower surface area ceria showed little evidence of ceria reduction under treatment, since the signal was largely masked by the high percentage of bulk ceria, which reduces above 700 °C. Since XANES averages over all cerium atoms (bulk + surface) and only surface ceria reduces at lower temperatures, a high surface area ceria is required to detect changes due to the surface reduction.

XRD patterns for the calcined support and catalysts are shown in Fig. 2. Integral breadth analysis using the Winfit 97 program [17] for the peak at 28.8° corresponding to (1 1 1) indicated that the domain size of the ceria was approximately 8.4 nm. The loadings of all metals were very low, and therefore, the particle sizes were too small to give corresponding metal oxide peaks that could be fitted. However, a small peak was found in the case of the Au and Ni catalysts.

TPR profiles reported in Fig. 3 show two important features. By comparing the reduction profiles of sintered ceria and HSAUP ceria, the bulk ceria is assigned to reduction at close to 750 °C. Reduction of the surface shell of ceria, present as a large broad peak on the high surface area ceria support, occurs between 400 and 500 °C. The metal function catalyzes and therefore shifts the peak for the reduction of the surface shell of ceria to lower temperatures, but has little effect, if any, on the bulk. The gold promoter shifted the surface ceria reduction to the lowest temperature. Platinum, copper, and nickel also displayed important shifts. Cobalt and iron were less effective. In addition to hydrogen consumption, the TPR peaks apparently contain a contribution from the decomposition of a surface species (perhaps a carbonate) as suggested by the DRIFTS spectra.

3.2. In situ XANES

A complete discussion of the in situ XANES results are reported elsewhere [16], but some information is repeated here for clarity. The XANES spectra were taken at the L_{III}-edge of cerium (5732 eV). In examining the reference spectra displayed in Fig. 4a, strong B_1 and C peaks occur at CeO_2. Peak C has been assigned to absorption into the 5d level with no occupancy in the 4f level, while B_1 is assigned to absorption into the 4f level (final state) [18,19]. After reduction to Ce^{3+}, peak B_o becomes apparent at an energy below that of B_1, and is associated with 4f occupancy in the initial state [18,19]. Representative XANES spectra for both Ce^{3+} and Ce^{4+} reference compounds are provided in Fig. 4a. The peaks provide an important fingerprint for the oxidation state of ceria after reduction treatment. Since only surface reduction can occur at low temperatures and XANES averages over both the bulk and surface, the catalysts display a mixture of both Ce^{3+} and Ce^{4+} contributions after surface reduction. That is, we observe a pronounced decrease in peak C and an increase in B_o relative to the unreduced CeO_2 reference. Fig. 4b and c indicates that there is surface reduction of the Pt/ceria catalyst after heating the catalyst under a hydrogen/nitrogen

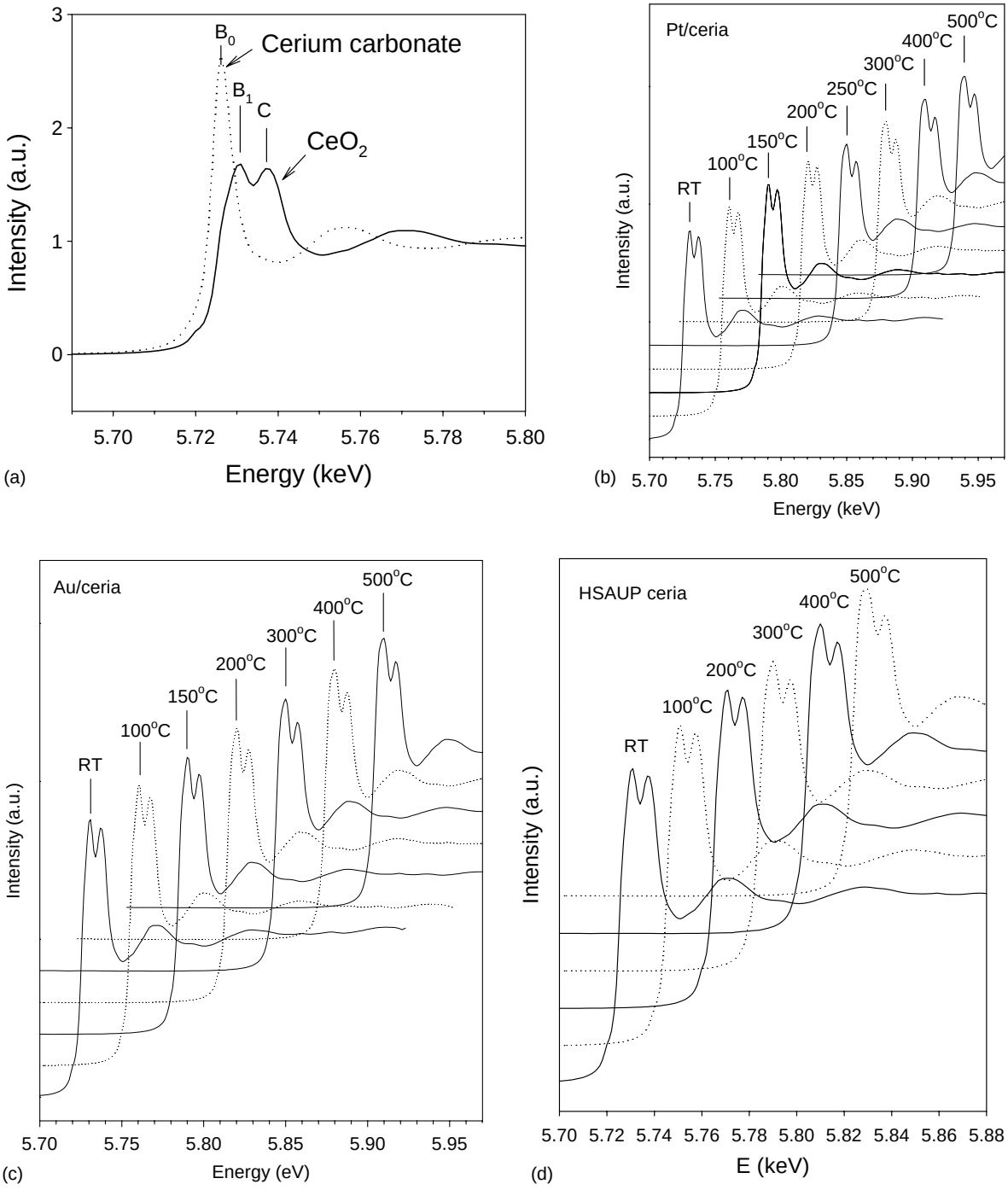

Fig. 4. (a) Normalized XANES spectra of (a) reference compounds, (b) the reduction of 1% Pt/CeO_2 in hydrogen, (c) the reduction of 1% Au/CeO_2 in hydrogen, (d) for the reduction of CeO_2 in hydrogen.

mixture to 250 °C, and the surface reduction occurs at even lower temperature for the Au/ceria catalyst. That the metal catalyzes surface reduction is evident by comparing the changes of the Pt/ceria catalyst with those of the unpromoted in Fig. 4d, where the surface reduction is complete at 500 °C. The temperatures of surface reduction are consistent with the TPR profiles. Linear combination (LC) fitting of experimental spectra with references reported in [16] showed that the extent of ceria reduction was higher in the case of Pt than Au.

3.3. In situ DRIFTS studies

A schematic of the DRIFTS setup is shown in Fig. 3. Catalysts were first reduced under flowing H_2 (100 cc) and N_2 (135 cc), as displayed in Fig. 5a–d. There is the decomposition of a band at 1610 cm^{-1}, which is likely decomposition of a surface carbonate. We make this assignment based on two points. There are no C–H stretching vibrations at 2850 cm^{-1} or 2940 cm^{-1} associated with this

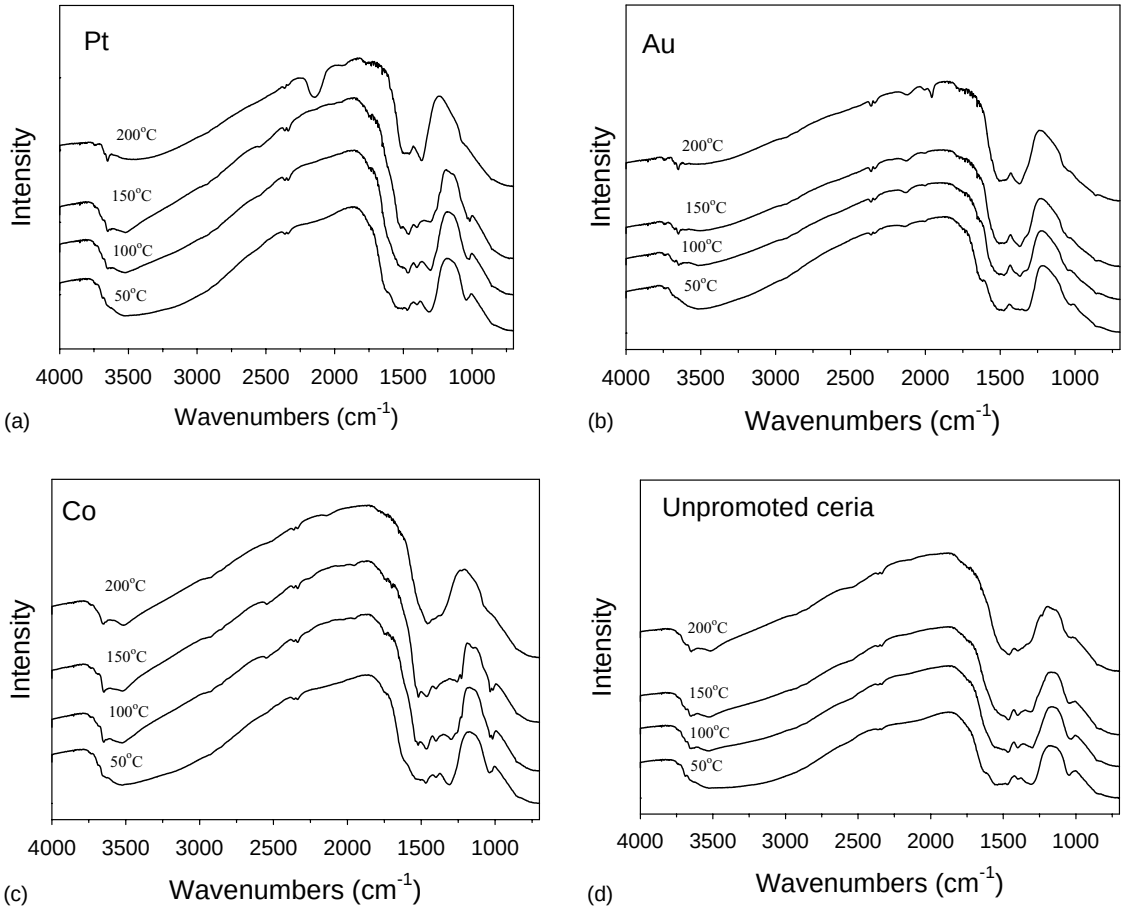

Fig. 5. (a) DRIFTS single beam spectra of the reduction of Pt/ceria with increasing temperature. Moving upwards: 50, 100, 150, and 200 °C. Strong geminal OH bands emerge after surface reduction for the case of Pt (100 cc H_2:135 cc N_2, 15 mg catalyst). (b) DRIFTS single beam spectra of the reduction of Au/ceria with increasing temperature. Moving upwards: 50, 100, 150, and 200 °C. OH bands emerge after surface reduction for the Au/ceria catalyst, but the intensity was weaker than for Pt (100 cc H_2:135 cc N_2, 15 mg catalyst). Cu catalyst was similar to Au. (c) DRIFTS single beam spectra of the reduction of Co/ceria with increasing temperature. Moving upwards: 50, 100, 150, and 200 °C. Weak geminal OH bands emerge after surface reduction for the Co and Fe promoted catalysts (100 cc H_2:135 cc N_2, 15 mg catalyst). (d) DRIFTS single beam spectra of the reduction of unpromoted ceria with increasing temperature. Moving upwards: 50, 100, 150, and 200 °C. Geminal OH bands very weak (100 cc H_2:135 cc N_2, 15 mg catalyst).

OCO vibration indicating a formate species. Also, as the band decomposes at higher temperatures during reduction, metal–CO and ceria–CO bands appear and decrease over time with desorption. Most importantly, for the metal promoters which are effective for catalyzing the surface reduction of ceria, the reduction is accompanied by the formation of sharp geminal OH vibrations at 3650 cm^{-1}, in agreement with the work of Shido and Iwasawa [9,10]. This is a critical point when comparing the catalysts. By comparing the width of the bands remaining between 1000 and 2000 cm^{-1} (i.e. the OCO stretching region) after hydrogen reduction at 200 °C, the removal of the surface species is most effective for the Group 10 metal Pt and Ni catalysts (Fig. 5a), followed by the Group 11 metal Cu and Au catalysts (Fig. 5b), then Fe and Co (Fig. 5c), and finally, the unpromoted catalyst (Fig. 5d). Representative spectra from each set are shown in Fig. 5a–d for the sake of brevity. Modification of bands in the carbonate region by H_2 reduction was also observed in a previous study [20]. The extent of formation of geminal OH groups on the reduced ceria surface followed the same trend. This is consistent with the idea that the active geminal OH groups occur on the reduced ceria surface.

After reduction, the cell was purged with flowing N_2 at 200 °C prior to adsorption of CO (3.75 cc) in 135 cc N_2. Fig. 6 shows that bands for surface formates and metal–CO evolved on the surface of the catalyst. Figs. 6 and 7 highlight the changes that occur with CO addition. In the OCO region (Fig. 6), symmetric and asymmetric OCO bands evolve. The asymmetric OCO band has been reported by Holmgren et al. [21] at 1580 cm^{-1} and the symmetric at 1375 cm^{-1}. We have observed in previous work that formates only evolve on reduced ceria surface by reaction of CO with the active geminal OH groups, and do not appear after low-temperature reduction for the unpromoted catalyst [16], but do appear upon CO addition after higher temperature (500 °C) reduction and cooling. Since the metal catalyzes the surface shell reduction, the bands appear at lower temperatures for the metal/ceria catalysts than for unpromoted ceria. We also do

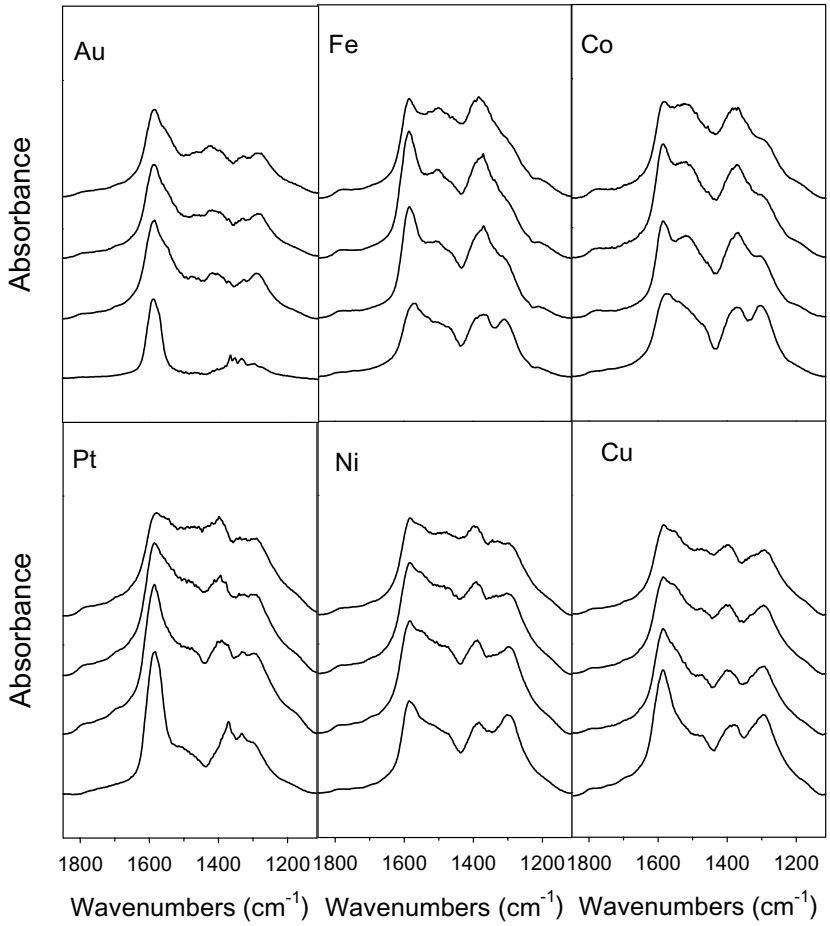

Fig. 6. DRIFTS difference spectra of the adsorption of CO to metal/ceria catalysts to yield surface formates (moving upward, reduced at 200, 250, 300, and 350 °C, respectively, and purged with nitrogen). Conditions: 3.75 cc CO:135 cc N_2, 15 mg catalyst. O–C–O stretching region.

not rule out the possibility of surface carbonates in this region in addition to the formate bands.

The formation of OCO bands of formates are accompanied by C–H stretching bands at 2840 and 2945 cm^{-1} (Fig. 7). These bands provide the key for understanding the mechanism since geminal OH and OCO formate bands are largely masked by gas phase water vibrations under in situ water-gas shift. As displayed in the figure and in our previous work, when high H_2O/CO ratios are utilized (i.e. first order dependency for P_{CO} and zero order for P_{water}), the bands are limited by the water-gas shift rate, and in general, become more rate limited with increasing temperature, as expected for a surface intermediate. More precisely, though, it is important to compare the catalysts at each temperature. At 200 °C, the Pt, Au, and Cu were most effective in catalyzing the reduction of surface ceria at the low temperature. At about 250 °C, as described in our previous XANES study [16], the extent of ceria reduction was higher with Pt than Au. Likewise, the intensity of geminal OH bands were highest for the Group 10 Pt and Ni catalysts after reduction at 250 °C. This follows, since surface reduction is required to generate the active geminal OH groups and the Group 10 Pt and Ni metals result in a greater extent of surface reduction. Group 11 Au and Cu yielded lower, but similar, geminal OH intensities, after reduction at 250 °C. This is consistent with the lower extent of surface reduction found for Au in XANES.

The active geminal OH groups on reduced ceria surface react with CO to produce formates. Fig. 7 shows that, at 200 °C, addition of CO gave the highest intensity of formate C–H stretch bands for Pt, followed by Au and Cu. However, the intensities for Ni, Co, Fe, and the unpromoted samples remained very low, since the catalysis of surface ceria reduction did not take place at the low temperature to give the active geminal OH groups. However, reduction at 250 °C resulted in ceria surface reduction for Ni and, less so, for Co and Fe, resulting in the generation of more geminal OH groups on the partially reduced surface. Therefore, addition of CO at 250 °C resulted in increases in formate band intensities for Ni, Co, and Fe. In contrast, surface ceria reduction was already complete by 200 °C for Pt, Au, and Cu (though a deeper reduction evident for Pt relative to Au from XANES). Therefore, for Pt, Au, and Cu, at 250 °C, addition of CO results in a decrease in band intensity relative to the 200 °C condition, consistent with the newly established adsorption/desorption equilibrium. Using a similar

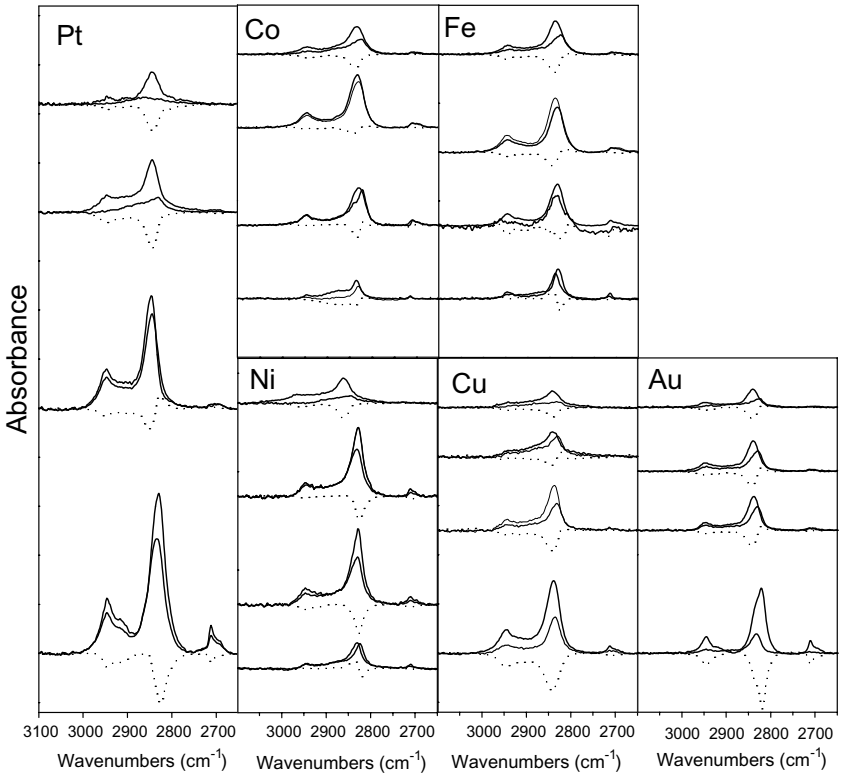

Fig. 7. DRIFTS difference spectra of the adsorption of CO to metal/ceria catalysts to yield surface formates (moving upward, reduced at 200, 250, 300, and 350 °C, respectively, and purged with nitrogen). Conditions: 3.75 cc CO:135 cc N_2, 15 mg catalyst. Replacing N_2 with 125 cc water to conduct WGS limited the formate bands, and difference (negative dotted bands) C–H stretching region.

line of reasoning, at the 300 °C condition, there are further increases in formate band intensity with addition of CO for the Co and Fe catalysts due to the reduction of more surface ceria at that temperature (generating more geminal OH groups on the ceria surface) (Fig. 8). For the other metals, surface reduction was already completed, so the formate intensities are lower relative to the 250 °C condition, due to the newly established adsorption/desorption equilibrium at 300 °C.

The Pt and Ni Group 10 metal catalysts were most effective in promoting the rate of the WGS reaction at and above 250 °C. The formate bands were, in general, higher under adsorption of CO alone. Under steady state WGS, the formates were reaction rate limited, especially at the higher temperatures (and therefore, conversions), as expected for surface intermediates. Au and Cu Group 11 metal catalysts gave similar responses to CO addition as Pt at each temperature, but the formate C–H intensities were much lower. This is consistent with the XANES results, which showed that Pt gave a deeper reduction of ceria surface than Au, resulting in higher geminal OH band intensities, and therefore, higher formate concentrations upon addition of CO.

Fig. 9 highlights the changes in geminal OH group intensity after adsorption of CO at each temperature. Important changes were revealed at each temperature as a function of the density of geminal OH groups present. Again, this is directly related to the degree of surface ceria reduction. That

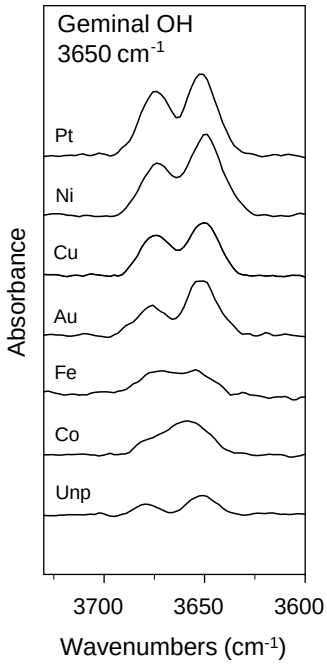

Fig. 8. Extent of geminal OH group formation after reduction at 250 °C. Establishes link between effectiveness of reduction promoter in catalyzing surface reduction and generation of the active geminal OH groups.

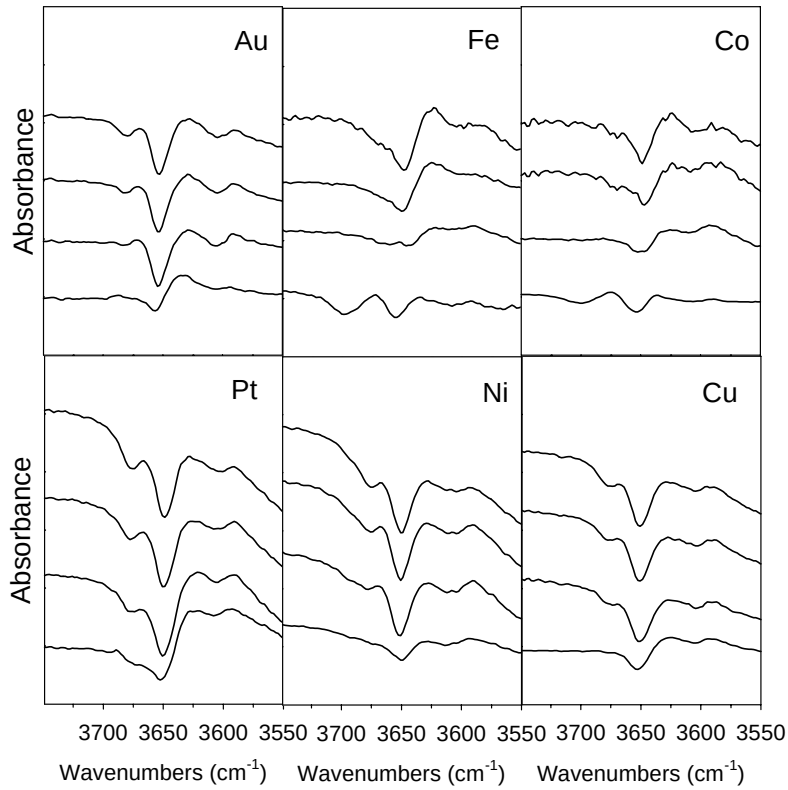

Fig. 9. Change in geminal OH group intensity after CO adsorption after moving upwards at 200, 250, 300, and 350 °C, respectively.

is, Pt, Au, and Cu showed important decreases in geminal OH with CO adsorption at 200 °C, Ni at 250 °C, and Co and Fe at higher temperature.

3.4. Reactivity

Results of reaction testing are displayed in Figs. 10 and 11. Catalysts were run in the fixed bed reactor at conditions which were designed for testing low-temperature water-gas shift catalysts as used in a fuel cell reformer. The conditions were: 100 ccm of hydrogen, 3.75 ccm CO, 125 ccm water, and 10 ccm of nitrogen. The amount of catalyst utilized was 0.66 g. Temperatures utilized were 250 °C, 300 °C, and 350 °C. The Pt catalyst was so active, that the catalyst amount had to be lowered to 0.033 g (a factor of 20) to reveal the lightoff curve (see Fig. 11). The reactivity for the first series including Pt, Ni, Co, Fe, and unpromoted gave a trend that followed the effectiveness of the promoter in shifting the ceria surface reduction catalysis to lower temperatures. Therefore, the trend was Pt > Ni > Fe > Co > unpromoted. Pt was also found to give a deeper reduction relative to Au, and presumably, Cu, as it behaved very similarly to Au. Not surprisingly, the Pt catalyst displayed much higher activities (about a factor of 20) relative to the Group 11 metals.

Shido and Iwasawa previously attributed the higher WGS rate on Rh/ceria in comparison to unpromoted ceria to a forward promotion of the rate by water, leading to the reactant-promoted mechanism. In agreement with their work, we have also verified a kinetic isotope effect which is likely associated with water decomposing the surface formate. Therefore, the ability of water to aid in reducing the activation energy barrier for the Rh/ceria is certainly a plausible possibility. However, one should also take into account the increase in geminal OH groups (the active sites), which occur on reduced ceria surface, as a consideration. Since the metal catalyzes the surface reduction, the active geminal OH groups occur at lower temperatures than for the unpromoted catalyst.

Interestingly, our studies have been in contrast to work that supports the ceria-mediated redox mechanism. As mentioned before, we believe that the surface carbonates reported at high CO/H_2O ratios previously are likely formates. Claims that carbonates deactivate the mechanism seem therefore highly speculative at this time. Ghenciu [4] recently reported a decrease in the BET surface area with ceria crystallites under reaction as a deactivation mechanism, and indicated that another mechanism may be operating in additional to the ceria-mediated redox process. Loss of ceria surface would certainly be in line with the active site (geminal OH groups) being on the reduced ceria surface. This is again in contrast to the ceria-mediated redox mechanism, where the active site is the interaction between metal and ceria. In fact, this is a critical point. However, we do not rule out the possibility that Pt may also agglomerate with loss of ceria surface area claimed. The authors supporting

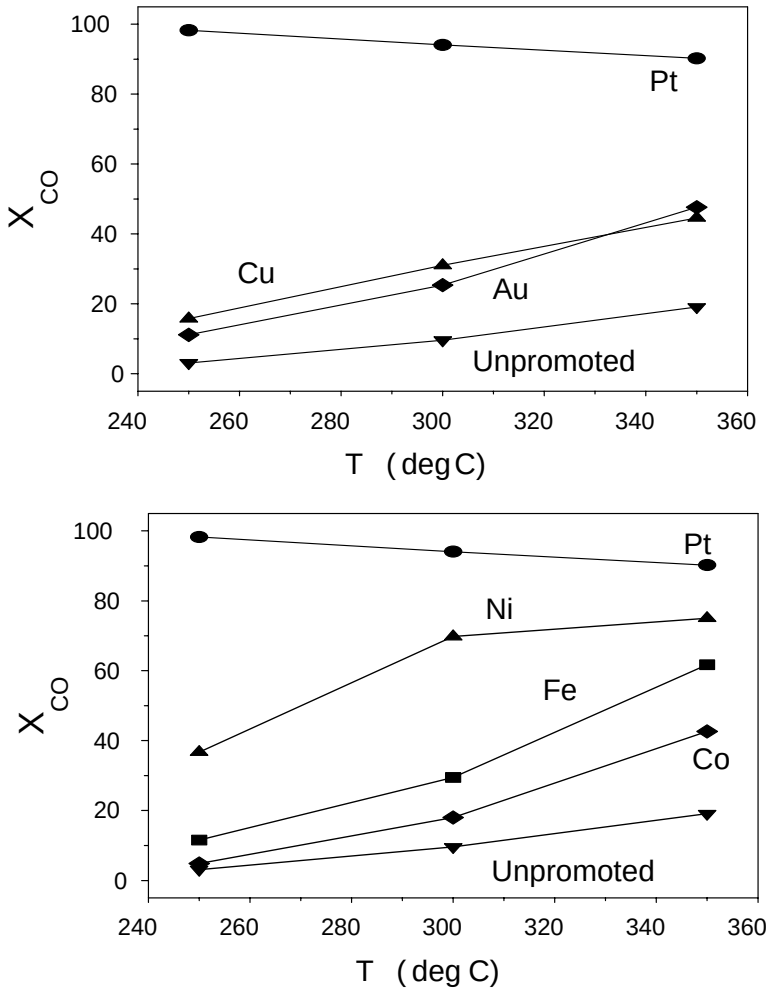

Fig. 10. Catalyst testing in the fixed bed reactor (3.75 cc CO, 100 cc H_2, 125 cc water, and 10 cc nitrogen, 0.66 g catalyst). Bottom: Comparison of typical promoter metals. Top: Comparison of group 11 metals. GHSV = 21.7 l/(g cat h).

a redox mechanism [5–8] cite these catalysts as supported metal catalysts, whereas we refer to them as metal-promoted ceria. Changes to the ceria support were also hypothesized to be responsible for the deactivation pattern of Pt/ceria catalysts in another, more practical, study, where conditions used were much closer to those used in a fuel cell reformer [22]. In that case, overreduction was claimed. Based on this investigation, Pt is certainly important from the standpoint of activity for these catalysts. We do not rule out the possibility at this time that Pt may have a direct role in the mechanism, but one role is to catalyze the surface reduction of ceria to create the active geminal OH groups on the surface. If Pt is involved in the mechanism, it should somehow be related to the decomposition of the surface formate.

Since all of our results indicate that maintaining reduced ceria surface is important for stability, we are currently incorporating refractory materials into the ceria to prevent sintering. We are currently examining modifiers, including zirconia, lanthana, neodymium, and praeseodymium, that were important stabilizers for ACCC catalysts.

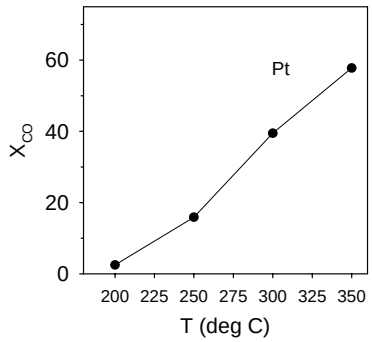

Fig. 11. Catalyst testing in the fixed bed reactor (3.75 cc CO, 100 cc H_2, 125 cc water, and 10 cc nitrogen, 0.033 g catalyst) for Pt/ceria catalyst. GHSV = 434 l/(g cat h).

4. Conclusions

One important function of the metal was to catalyze the reduction of the surface ceria. This not only involves the

shifting of the reduction temperature to lower temperature, but also the extent of reduction. The surface reduction is critical for generating the active geminal OH groups on the surface of the ceria. Addition of CO yielded surface formates by reaction with the geminal OH groups. Water addition then decomposed the formates to give the products of reaction, in agreement with our previous studies. DRIFTS indicated that the Pt/ceria catalyst yielded strong geminal OH bands after reduction at low temperature, and the catalyst was about an order of magnitude more active in the temperature range studied than the other metal/ceria catalysts studied. Au and Cu also catalyzed the surface reduction to low temperatures, but the extent of reduction was lower. Geminal OH groups were less intense after reduction, and the catalysts were less active than Pt. TPR showed that Ni, and moreso, Fe and Co, catalyzed surface reduction at a higher temperature than that of Pt. Therefore, geminal OH formation increased with reduction temperature, and the increased site densities were reflected in the rates found from testing in the fixed bed reactor.

Acknowledgements

The work was supported by the Commonwealth of Kentucky. Special thanks to Dr. Syed Khalid (Beamline X18b) for help with XANES, Joel Young for XAS cell construction.

References

[1] Fuel Cell Handbook, fifth ed., US DOE, NETL, 2000.
[2] Fuel Cells for Transportation Program Contractors' Annual Progress Report, US DOE, OAAT, 1998.
[3] D.C. Dayton, M. Ratcliff, R. Bain, Fuel Cell Integration—A Study of the Impact of Gas Quality and Impurities, NREL/MP-510-30298, 2001.
[4] A.F. Ghenciu, Curr. Opin. Solid State Mater. Sci. 6 (2002) 389–399.
[5] T. Bunluesin, R. Gorte, G. Graham, Appl. Catal. B 15 (1998) 107.
[6] S. Hilaire, X. Wang, T. Luo, R.J. Gorte, J. Wagner, Appl. Catal. 215 (2001) 271.
[7] Y. Li, Q. Fu, M. Flytzani-Stephanopoulos, Appl. Catal. B 27 (2000) 179.
[8] Q. Fu, A. Weber, M. Flytzani-Stephanopoulos, Catal. Lett. 77 (1–3) (2001) 87.
[9] T. Shido, Y. Iwasawa, J. Catal. 141 (1993) 71.
[10] T. Shido, Y. Iwasawa, J. Catal. 136 (1992) 493.
[11] J.C. Lavalley, Catalysis Today 27 (1996) 377.
[12] Y. Amenomiya, I.T. Ali Emesh, K.W. Oliver, G. Pleizier, in: M.J. Phillips, M. Ternan (Eds.), Proceedings of the 9th International Congress on Catalysis, vol. 2 (C1 Chemistry), Chemical Institute of Canada, Ottawa, Ont., Canada, 1988, p. 634.
[13] G. Jacobs, L. Williams, U. Graham, D. Sparks, B.H. Davis, J. Phys. Chem. B 107 (2003) 10398.
[14] G. Jacobs, L. Williams, U. Graham, D. Sparks, G. Thomas, B.H. Davis, Appl. Catal. A: Gen. 252 (2003) 107.
[15] G. Jacobs, P.M. Patterson, L. Williams, E. Chenu, D. Sparks, G. Thomas, B.H. Davis, in: Proceedings of the 18th NAM, Cancun, Mexico, June 2003.
[16] G. Jacobs, P.M. Patterson, L. Williams, E. Chenu, D. Sparks, G. Thomas, B.H. Davis, submitted for publication.
[17] S. Krumm, Winfit 97, Version 1.2.1, June 1997.
[18] S. Overbury, D. Huntley, D. Mullins, G. Glavee, Catal. Lett. 51 (1998) 133.
[19] J. El Fallah, S. Boujani, H. Dexpert, A. Kiennemann, J. Marjerus, O. Touret, F. Villain, F. Le Normand, J. Phys. Chem. 98 (1994) 5522.
[20] A. Laachir, V. Perrichon, A. Badri, J. Lamotte, E. Catherine, J.C. Lavalley, J. El Fallah, L. Hilaire, F. Le Normand, E. Quemere, G.N. Sauvion, O. Touret, J. Chem. Soc., Faraday Trans. 87 (1991) 1601.
[21] A. Holmgren, B. Andersson, D. Duprez, Appl. Catal. B 22 (1999) 215.
[22] J.M. Zalc, V. Sokolovskii, D.G. Loffler, J. Catal. 206 (2002) 169.